International Journal of Bioelectromagnetism
Vol. 9, No. 4, pp. 253 – 259, 2007

www.ijbem.org

Removal of ocular artifacts for high-resolution EEG studies: a simulation study

Laura Astolfi [b,g], Febo Cincotti [b], Donatella Mattia [b], Maria Grazia Marciani [b], Fabrizio De Vico Fallani [d,b], Fumikazu Miwakeichi [e], Yoko Yamaguchi [f], Pablo Martinez [a], Serenella Salinari [g], Andrea Tocci [b], Hovagim Bakardjian [a], Andrzej Cichocki [a] and Fabio Babiloni [c,b],

a La a *Laboratory for Advanced Brain Signal Processing Riken, Brain Science Institute, Japan*

b *IRCCS "Fondazione Santa Lucia", Rome, Italy*

c *Dipartimento di Fisiologia umana e Farmacologia, Rome, Italy*

d *Centro di Ricerca de "La Sapienza" per l'Analisi dei Modelli e dell'Informazione nei Sistemi Biomedici, Rome,Italy*

f L*aboratory for Dynamics of Emergent Intelligence, Riken, Brain Science Institute, Japan*

e *Department of Medical System Engineering, Faculty of Engineering, Chiba University, Japan*

g *Dep. of Informatica e Sistemistica, Univ. of Rome "La Sapienza", Rome, Italy*

Abstract. Eye movements and blinks may produce unusual voltage changes that propagate from the eyeball through the head as volume conductor up to the scalp electrodes, generating severe electroencephalographic artifacts. Several methods are now available to correct the distortion induced by these events on the EEG, having different advantages and drawbacks. The focus of this work is to quantify the performance of the removal of EOG artifact due to the application of the independent component analysis (ICA) methodology. The precise quantification of the effects of artifact removal by ICA is possible by using a simulation setup, with a realistic head model, that it is able to mimic the occurrence of an eye blink. The electrical activity generated by the simulated eye blink were propagated through the realistic head model and superimposed to a clean segment of EEG. Then, artifact removal was performed by using the ICA approach. Ocular artifact removal was evaluated in different operative conditions, characterized by different Signal to Noise Ratio and number of electrodes. The error measures used were the Relative Error and the Correlation Coefficient between the clear, original EEG segment and those obtained after the application of the ICA procedure.

Keywords: EOG, EEG, ICA, realistic head model, high resolution EEG

1. Introduction

Nowadays, it is well know that high resolution EEG is a body of techniques based on the use of realistic head models that allow to estimate the activity of cortical areas from non invasive EEG recordings performed with a high number of electrodes (64-256). Despite the important amount of information estimated from high resolution EEG recordings the main problem that remains in the interpretation of such cortical activity is the dependence of the estimated activity from the different sources of artifacts. In fact, often-complex neurophysiologic tasks require the overt verbalizations of the subjects or the explicit movement of the eyes along the presented pictures. These verbalizations or eye movements generate muscle activities that are represented in the frequency spectra of the gathered EEG signals. The estimation of the cortical current density will be heavily affected by the occurrence of these ocular artifacts on the EEG data In fact, subtle eye movements involved in even well-controlled tasks, generate over the frontal areas scalp potential artifacts that can be projected by the linear procedures on cortical areas located frontally. The origin of such artifacts is due to the potential difference existing through the eyeball (between retina and cornea) which during blinks is shortcut, generating a signal that propagates through the volume conduction arriving to the scalp sensors. Such signal, which is measured by the electrooculogram [1], causes a potential shift on the scalp surface. A simplified model of such blink assumes an electric dipole within the eyeball and a spherical model for the head as a volume conductor [2]. The occurrence on the scalp electroencephalogram (EEG) of the electrical artifacts generated by eye movement is a well recognized problem in EEG-based studies. To correct, or remove the ocular artifacts from the EEG, many regression-based techniques have been developed in both time and frequency domains [3]. More recently, component-based techniques, such as principal component analysis (PCA) and independent component analysis (ICA; [4]), have also been proposed to remove the ocular artifacts from the EEG. The use of the ICA, Blind Source Separation (BSS) and Parallel Factor Analysis (PARAFAC) methods to remove appropriately the sources of artifacts in the EEG or MEG or even fMRI have been adequately underlined in previous studies [5-6]. ICA/BSS techniques have been successfully applied to remove artifacts and noise including background brain activity, electrical activity of the heart, eye-blink and other muscle activity, and environmental noise efficiently. It is worth notice that most of the methods require manual detection, classification of interference components and the estimation of the cross-correlation between independent components and the reference signals corresponding to specific artifacts [4-6]. However, recently, some attempts have been made to remove the ocular artifacts by using automatic classification techniques using a BSS approach [7]. Whatever the method is used for the removal or filtering the EOG artifacts from the EEG waveforms, the central issue is how this method works in different operative conditions related to the Signal To Noise Ratio (SNR) and the number of electrodes used for the EEG data collection.

The aim of the present study was to characterize the efficacy of the artifact removal algorithm based on the BSS from high-resolution EEG recordings. In particular, we reached this aim through a simulation study in which we were able to mimic the occurrence and the spread of generated eye blink artifacts on the synthesized scalp potentials, by using realistic head and cortical models for the approximation of the volume conductor properties. By using such simulation setup we estimate exactly the influence of blink artifacts over the different scalp electrodes EEG waveforms. Hence, we were in the situation to evaluate accurately the efficacy of the ThinICA procedure [5] in the removal of the EOG artifacts under different operative conditions, with variable SNR and number of sensors.

2. Material and Methods

Design of Test Datasets. An EEG dataset was designed to provide baseline measures that were used to compute statistical measures of efficacy of the ocular artifact removal by the ICA algorithm across the different conditions of SNR and number of electrodes employed. The EEG data segment, sampled at 250 Hz, was without blink artifacts occurrence and constituted the baseline data to which blink activity generated through the realistic head model was added.

The scalp leads. Three electrodes arrays shown in Fig.1 have been considered. The first one was with 19 electrodes disposed on the scalp surface according to match the 10-20 system with the frontal Fp1 and Fp2 electrodes included. The others have 64 and 31 electrodes.

The Signal to Noise Ratio (SNR). White noise was added to the EEG dataset, to reach five different levels of signal-to-noise ratios (SNRs: 1, 3, 5, 10, 100). This recalls the typical range of SNR commonly encountered in evoked, motor- and cognitive-related EEG recordings. The SNR expressed directly the ratio between the signal power and the noise power added to the EEG data, not using the decibel notation.

Realistic head model. T1-weighted MRIs were employed. Scalp, skull, compartments were segmented from MRIs and tesselated with about 5000 triangles for each surface. The eyeballs were also segmented and two free rotating dipoles were placed within such structures (Fig 1, D). By changing the time-varying moment of such dipoles, the eye blink was simulated in such a way the propagation of the electric field to the frontal scalp leads Fp1 and Fp2 generates a correlation superior to 0.99 with the eye blink really recorded from the subject whose head was employed for the realistic head model. The time-varying strength profile of the current dipoles simulating the eye blink was then used in the successive simulations. Afterwards a succession of blinks was generated, by repeating the profile of current strengths for the two employed dipoles inside the head model. The occurrence of such blinks were not regularly spaced in time, and 12 occurrence of them will be generated. Such blinks were thereafter propagated and added linearly to the EEG waveforms on the leads on the realistic head model. The EEG presented different values of SNR and were analyzed by using different montages, as previously described. With this procedure, several EEG datasets contaminated by EOG were available, with different SNRs and number of electrodes. On each one of such EEG datasets the Thin ICA algorithm [5] was applied and the component related to the eye blinks were located and removed. At least 50 EEG dataset related to each condition of SNR level and for a predetermined number of electrodes montage were generated for the successive statistical analysis.

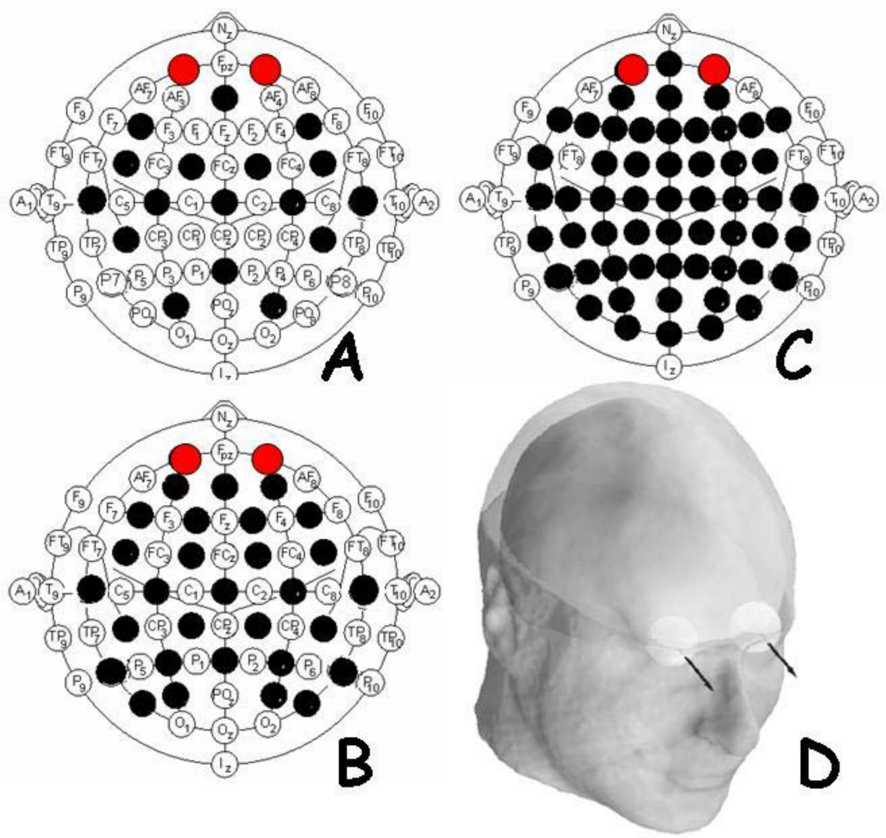

Figure 1. *A, B, and C represents three montages used in the simulation. The head is seen from above, the nose up. The black dots represent the electrodes effectively used in the simulations; the white circles represent the location of the extended 10-20 International System. Panel D shows the realistic reconstruction of the head with the dipoles used to mimic the generation of the blink placed in the eyeball.*

After applying ThinICA algorithm to these test data, the cleaned data were compared directly with the baseline EEG, to provide quantitative as well as qualitative measures of ThinICA failure or success. By design, the simulated blink activity is the projection of a single, independent, uncorrelated component. A single component from each ThinICA decomposition should therefore cleanly recapture it. Failure can then be partly measured by the extent to which blink activity is not recaptured by a single component, indicating a weakness in how the respective ThinICA algorithms measured and approximated independence or maximal temporal decorrelation. This problem is also known as “blink splitting”.

The dependent variables used. In the different experimental conditions, the similarity of the “eyeblink corrected” EEG waveforms array (**Es**) with the clean original EEG dataset one (**Gs**) has been evaluated by computing two indexes, to be used in the simulations as dependent variables. The first one is the correlation coefficient (Cc) between the generated and the estimated average source waveforms, according to the formula:

$$\mathbf{C}c = \frac{\mathbf{Gs} \bullet \mathbf{Es}}{\sqrt{\|\mathbf{Gs}\|_2^{\,2} \cdot \|\mathbf{Es}\|_2^{\,2}}} \tag{1}$$

where · stands for the usual inner products between the **Gs** and the **Es** vectors. The second one is the relative error (RE), computed according to the formula:

$$\mathrm{RE} = \|\mathbf{Gs}\text{-}\mathbf{Es}\| / \|\mathbf{Gs}\| \tag{2}$$

where $\|\mathbf{x}\|$ is the standard L2 norm of a vector $\mathbf{x}$.

The statistical analysis. The obtained results were subjected to separate Analysis of Variance (ANOVA). The main factors of the ANOVAs were the SNR (with five levels: 1, 3, 5, 10, 100) the number of electrodes of the recording array (ELECTRODES, with three levels: 19, 31 and 64) and the position of the electrodes (POSITION, with two levels, Fp1 and Fp2). Separate ANOVAs were performed on Cc and RE data. In all the evaluated ANOVAs, the correction of Greenhouse-Gasser for the violation of the spherical hypothesis was used. The post-hoc analysis with the Scheffe's test at the p = 0.05 statistical significance level was then performed**.**

3. Results

According to the experimental design, the RE variable was measured and subjected to the ANOVA including the SNR, ELECTRODE and POSITION factors. Results revealed a strong influence of the main factors SNR (F = 205, p<0.0001), ELECTRODES (F=1190, p<0.0001), and POSITION (F=29, p<0.0001), as well as their interactions. Of interest is the interaction between all the factors SNR x ELECTRODES x POSITION (F=28, p<0.0001), on the Relative Error variable. Fig. 2 shows the average plots of the influence of the levels of the main factors SNR, ELECTRODES and POSITION on the RE In particular, Fig. 2 shows that for each increase in SNR of the EEG recordings, there is a decrease in the RE. The influence of the factor ELECTRODES is also significant, suggesting a benefic effect of the increasing the electrodes number for EEG recordings. Post hoc tests revealed that there were no significant differences between levels 3, 5, and 10 of the SNR factor for the POSITION levels, Fp1 and Fp2. The bar on each point represents the 95% confidence interval of the mean errors computed across the simulations. The data obtained for the other indexes obtained, the correlation coefficient (Cc) are represented in Fig. 3. The ANOVA performed returned again a strong influence of all the factors considered SNR, ELECTRODES and POSITION.

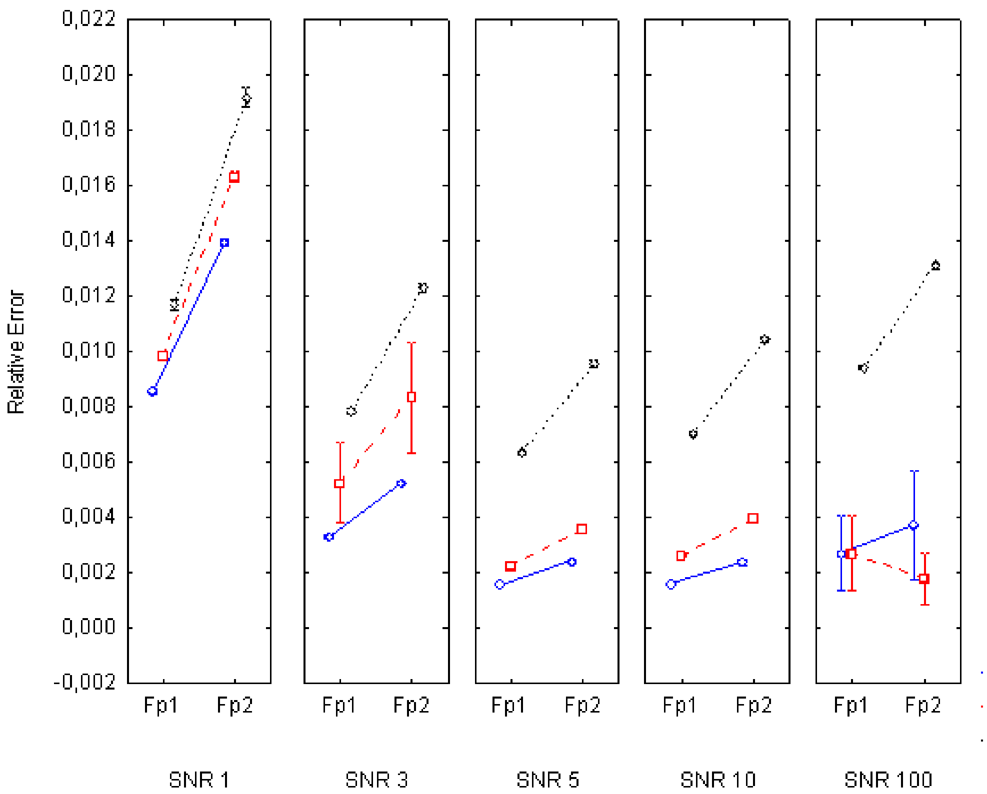

Figure 2. *Average values of the Relative Error (RE) obtained from the removal of EOG over the EEG waveforms in different conditions of SNR. Five panels are shown, each one relative to values of RE for SNR 1,3,5,10,100 (from left to right). Each color codes values of RE obtained for the montage at 19 electrodes (green, dotted line), 31 electrodes (red, thin line) and 64 electrodes (blue, continuous line). Two average data points are presented in each panel, one for the RE obtained at the Fp1 electrode location (left position on the panel) and for the Fp2 location (right position on the panel). It is possible to observe the lower values of the RE for increasing SNR as well as for increasing the number of electrodes used for the analysis. No statistical significant differences were noted between Fp1 and Fp2 removal for almost all the SNR level.*

The analysis of the local parameters also showed time-frequency varying distributions over the scalp. In Fig. 3, we have depicted the evolution of the local degree and network configuration for three different time instants (250 ms before and 250 and 750 ms after the presentation of the stimulus) and two selected frequencies (10 Hz and 18.5 Hz). Both, network indices and the topographical distribution of the local parameters over the scalp vary across time and frequency. It should be noted that, for the same time instant, the networks at different frequencies behave differently. 250 ms before the stimulus arrival, the network present a highly connected area in the parietal region at frequencies around 10 Hz, while for 18.5 Hz two regions (frontal and one more occipital) can be observed. After the stimulus arrival, the highly connected pattern of synchronization elicited at t ~ 250 ms for frequencies in the beta range is characterized by two clusters that are interconnected by long-range connections, marking a coordination between the two distant regions. After that, the processing of the stimulus reshapes completely the configuration of the local parameters; for the 18.5 Hz representation, the local degree decreases and the long-range connections disappear. For activities at 10 Hz topography, the frontal "activation" remains, while the parietal one disappears and new long-range connections are established from frontal to more occipital areas.

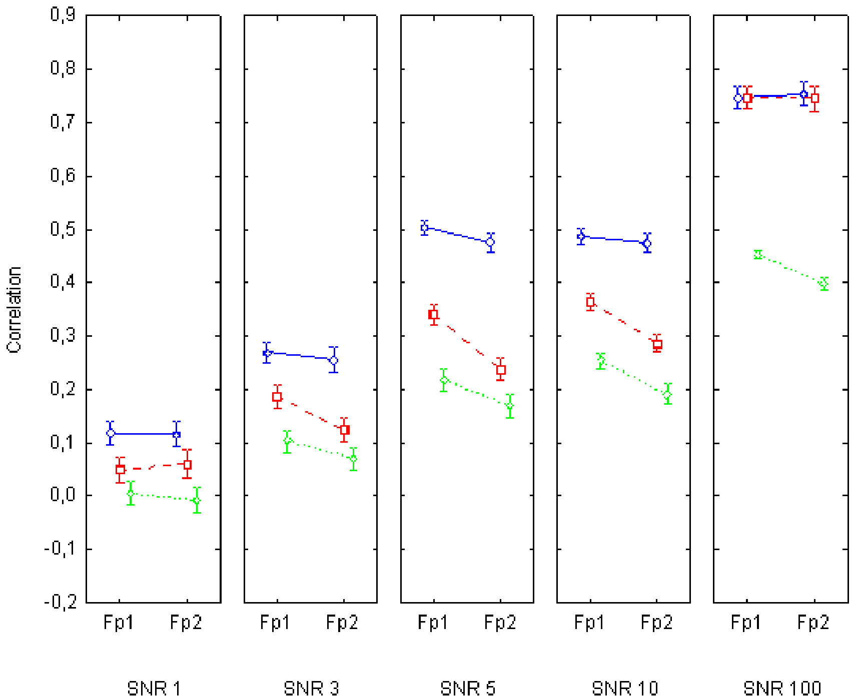

Figure 3. *Average values for the correlation coefficient (CC) between the original EEG and the filtered EEG after the ICA algorithm with the removal of the component related to the occurrence of the blink artifacts. Same conventions as in Figure 2. CC values increased by increasing the SNR levels, as well the number of electrodes. No statistical significant differences were noted between the electrodes Fp1 and Fp2.*

In particular, we have for the main factors SNR ($F = 2060$, $p<0.000001$), ELECTRODES ($F=1501$, $p<0.000001$), and POSITION ($F=105$, $p<0.0001$), as well as for the interactions. The SNR x ELECTRODES x POSITION is also statistically significant ($F=6$, $p<0.001$). Also in this case the Fig. 3 suggest the benefic effect on the removal of the EOG artifact from the EEG waveforms of an increasing SNR and number of electrodes, while the differences between the location (Fp1 and Fp2) are not constant through all the database.

4. Discussion

The neuroscientific community interested in the use of high resolution EEG methodologies to investigate the behavior of the human brain with a high temporal resolution would like to know "how" and "how much" it is possible to remove the possible sources of spurious activity deriving from the above mentioned non-brain activity from the recorded electromagnetic fields. Despite this clear question, it is striking to note the lack of simulation studies in the scientific literature in which the amount of artifacts induced in the ongoing EEG can be precisely stated, as well as the amount of corrections performed by the proposed algorithms. In fact, the word "simulation" appear in MEDLINE on papers related to the correction of EOG artifacts induced by eye movements on EEG or MEG measurements just in a couple of papers of Berg and Scherg of 1991[2], and from Wallstrom et al., 2004 [8]. Furthermore, in those papers, the simulations were performed without a systematic variation of the noise and amplitude parameters that characterized such artifacts in the real EEG/MEG recordings. This means that the efficacy and the efficiency of the different proposed methodologies able to recover from muscle or ocular artifacts in literature is mainly tested on real data, in which the amount of correct EEG is simply unknown, and the level of artifacts occurrence is untested.

The use of some quantitative indexes to address the efficacy of the EOG artifacts removal was produced in literature [9-11]. While the first compared the power spectral density of the original and reconstructed waveforms to measure the extent to which “artifactual” activity had been removed, the second computed the correlation coefficient between corresponding channels of the EEG before and after artifact removal. In this last case, a low correlation was an evidence of a successful artifact removal.

In the present case, the achievement of a high correlation implies that the EOG activity superimposed to the original EEG through the volume conductor was successfully removed. Regression-based EOG correction raises a major concern: as the EOG channel may pick up EEG activity, EEG activity may be removed too. This endorses the use of ICA algorithms on the removal of artifact correction due to the eye blinks.

The goal of the present research was to design a framework for objective (i.e., quantitative) evaluation of blink removal procedures, where success is defined as complete separation, and subsequent removal, of blink activity from multichannel EEG. Results suggest that under a large range of values for the SNR levels and different number of recording electrodes, the removal of eye blink by the ThinICA procedure return errors lower than 0.5% when 61 electrodes are used. However, it have to be noted that in such simulations we do not encountered the phenomena of the eye blink splitting, i.e. the split of the eye blink occurrence on the EEG waveforms in two or more independent components. This was probably due to the independent generation of the eye blink and the EEG dataset. Although this analysis has been performed actually only for the removal of eye blinks artifacts, by using the same setup the other sources of ocular artifacts can be studied and analyzed. Further work is then necessary to address properly the capability of the ThinICA algorithm to remove the EOG induced by horizontal and vertical eye movements onto the EEG.

Acknowledgements

This work was supported by a grant from RIKEN Institute, in collaboration with Laboratory for Advanced Brain Signal Processing
Riken, Brain Science Institute, WakoShi, Saitama, JAPAN. The COST NEUROMATH Action BM0601 also supported the work.

References

[1] Croft RJ, Barry RJ. Removal of ocular artifact from the EEG: a review. Neurophysiol Clin. 2000, 30(1):5-19.

[2] Berg, P. & Scherg, M. (1991a). Dipole modeling of eye activity and its application to the removal of eye artifacts from the EEG and MEG. *Clin Phys Physiol Meas, 12 Suppl A*, 49-54.

[3] Gratton, G., Coles, M. G. & Donchin, E. (1983). A new method for off-line removal of ocular artifact. *Electroencephalogr Clin Neurophysiol, 55*(4), 468-484.

[4] Jung, T. P., Makeig, S., Westerfield, M., Townsend, J., Courchesne, E. & Sejnowski, T. J.(2000). Removal of eye activity artifacts from visual event-related potentials in normal and clinical subjects. *Clinical Neurophysiology, 111*(10), 1745-1758

[5] Cichocki, A. & Amari, S. (2003). *Adaptive Blind Signal and Image Processing*. John Wiley & Sons

[6] Makeig S, Debener S, Onton J, Delorme A. Mining event-related brain dynamics. Trends Cogn Sci. 2004 May;8(5):204-10.

[7] Joyce, C. A., Gorodnitsky, I. F. & Kutas, M. (2004). Automatic removal of eye movement and blink artifacts from EEG data using blind component separation. Psychophysiology, 41(2), 313-325.

[8] Wallstrom, G. L., Kass, R. E., Miller, A., Cohn, J. F., & Fox, N. A. (2004). Automatic correction of ocular artifacts in the EEG: a comparison of regression-based and component-based methods. International Journal of Psychophysiology, 53, 105-119.

[9] Barbati, G., Porcaro, C., Zappasodi, F., Rossini, P.M., & Tecchio, F. (2003). Optimization of an independent component analysis approach for artifact identification and removal in magnetoencephalographic signals. *Clinical Neurophysiology, 115*, 1220-1232.

[10] Iriarte, J., Urrestarazu, E., Valencia, M., Alegre, M., Malanda, A., Viteri, C., et al. (2003). Independent component analysis as a tool to eliminate artifacts in EEG: a quantitative study. *Journal of Clinical Neurophysiology, 20*(4), 249-257

[11] O. Jahn, A. Cichocki, A. A. Ioannides, and S. Amari, "Identification and elimination of artifacts from MEG signals using efficient independent component analysis," in Recent Advances in Biomagnetism, Proceedings of the 11th International Conference on Biomagnetism (T. Yoshimoto, M. Kotani, S. Kuriki, H. Karibe, and N. Nakasato, eds.), (Sendai, Japan), pp. 224-227, Tohoku University Press, 1999.